HIGH SCHOOL EDITION
Journal of Student Research
Volume 14 Issue 1 (2025)

From Theory to Observational Results: Baryon Acoustic Oscillations Detected at High Redshift Ranges

Kevin Zhang[1] and Jiani Chen[#]

[1]Rock Ridge High School / Academies of Loudoun, USA
[#]Advisor

ABSTRACT

The current mission from several space science institutions occurring on a global scale is the search for baryon acoustic oscillation (BAO) peaks. In our work, we were able to successfully discover a BAO peak detected by the Dark Energy Spectroscopic Instrument (DESI) Early Data Release (EDR) at a higher redshift range than the current published work. In our study, we chose a selection of 60,431 quasars between redshifts ranges from $2 < z < 3$. We followed the methods used by current scientists which was to compute the correlation function, revealing a peak at roughly 110 h^{-1} Mpc at a significance value of $4 \cdot 10^{-73}$ compared to a correlation function associated with a pure CDM model. The detection of the BAO peak in the DESI EDR is significant as it shows the potential of DESI as a powerful tool to determine the BAO standard ruler across a wide range of redshifts, with the 2025 official DESI data release providing even more data to conduct in-depth studies on BAOs. Based on this result, future analyses can help refine the position of the BAO peak at high redshifts and uncover new values for cosmological parameters within the early universe.

Introduction

We have all heard of the Big Bang Theory as a physical theory that explains the expansion of the early universe, but this "big bang" has left echoes of sound waves from the nascent universe in the form of a characteristic pattern known as baryon acoustic oscillations (BAOs). In 2020, the National Aeronautics and Space Administration (NASA) released the James Webb Space Telescope which explored the primordial cosmic sea to observe the effects of these sound waves. Along with this mission to better understand baryon acoustic oscillations, other ongoing efforts for detecting BAO peaks include the Dark Energy Spectroscopic Instrument (DESI). DESI works as a ground-based observatory by taking in light from tens of millions of galaxies and other distant objects in the universe (Palanque-Delabrouille et al. 2021).

We can imagine the universe today, beyond our Milky Way Galaxy, resembling a jar of trail mix where when seen from a far, it has an anisotropic distribution. As depicted by a visualization created by NASA (Figure 1), our universe which is filled with clusters of galaxies and quasars (highly active, bright galaxies) truly looks like trail mix immersed in a molasses-like medium. As these cosmological objects move further away from each other, the light is shifted towards redder wavelengths. The data collected from DESI helps with understanding the repulsive force from "dark energy" that drives this expansion of the universe. BAOs serve as one of the probes for dark energy, and acquiring a deeper understanding on them as they ripple through the cosmos can also help provide us with a unifying theory of dark energy, dark matter, and baryonic matter (Chung, 2020). Furthermore, studying and understanding the nature and structure of baryon acoustic oscillations pose a tremendous feat for advancing human understanding of what the early universe was like when it was three billion years old.

In this research paper, we aim to provide an overview from theory to observational results of the current work in studying BAOs while also developing a computational framework for detecting baryon acoustic oscillation peaks.

Although scientists have set up the experimental apparatus for measuring and detecting BAOs through redshift surveys, not much work has been done for developing a general computational pipeline for detecting BAO peaks in a general redshift range. Through the usage of the DESI dataset, we will provide a first order approximate computation of the correlation to calculating BAO in a redshift range from 2 to 3 which is a higher range than the current work published by DESI (Moon et al. 2023). Furthermore, our pipeline aims to be adaptable for the next DESI dataset release so that further analysis can be made. The ability to easily detect BAO peaks for various redshift ranges can help scientists understand more about the way it influences galaxy distributions. While BAOs are artifacts from a turbulent era in the early universe, understanding their formation is important for detecting the characteristic peak at any redshift range. The location of this peak shows the way BAOs influenced the way quasars, are separated in the presence of dark matter.

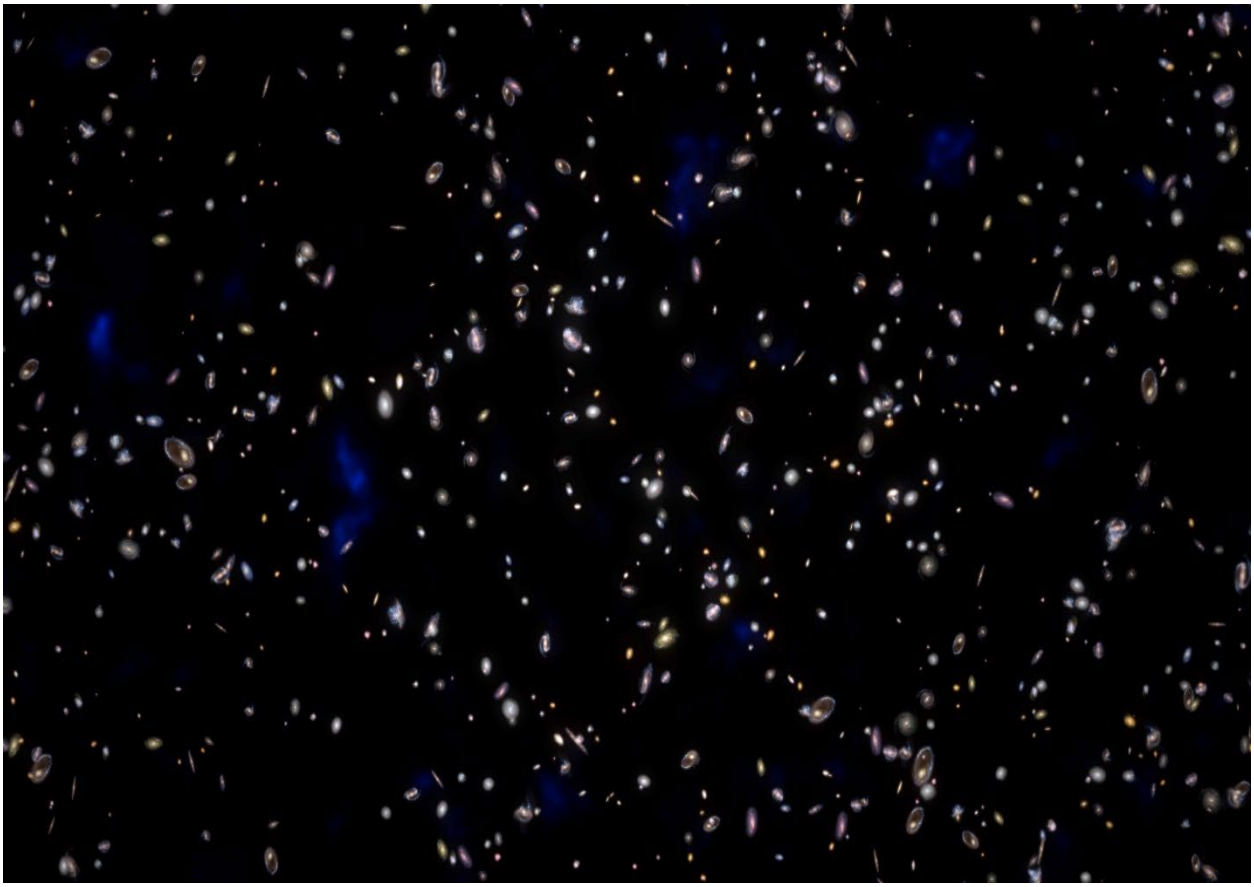

Figure 1. NASA visualization of the distribution of galaxies. The galaxies in the background resemble trail mix.

Theory

BAO Formation

BAOs were formed from baryon-photon interactions before photons decoupled, or ceased to interact, from baryons. Prior to photon decoupling at 380,000 years after the Big Bang, the early universe was made of a thick primordial plasma, a dense mix of protons, atomic nuclei, electrons, and photons. Neutrinos, tiny particles thousands of times less massive than an electron, were negligible in this state of the universe as they had decoupled, or ceased to interact

with, matter and radiation roughly one second after the Big Bang. Slight density anisotropies in the early universe led to the accumulation of dark matter and the plasma in areas where the universe was denser than the surrounding areas. This gravitational contraction led to an increase of outward radiation pressure caused by more baryon-photon interactions, leading to the production of sound waves at the source of the overdensity, traveling at half the speed of light.

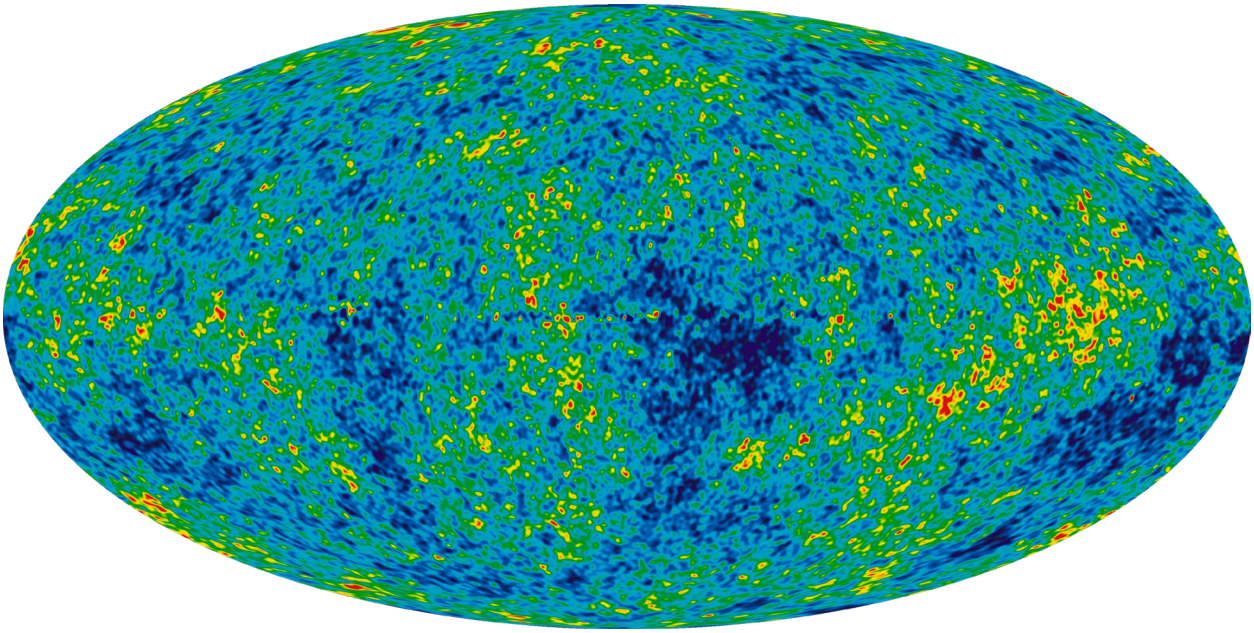

Figure 2. A visualization of the cosmic microwave background (CMB) as collected by the WMAP satellite. Red areas are slightly hotter areas while blue areas are slightly colder areas, corresponding to over- and underdensities, respectively.

At recombination and photon decoupling, the radiation-driven outward pressure disappeared as photons no longer interacted with baryonic matter, effectively freezing the BAOs in place. The photons that were emitted immediately after this event can be seen in the cosmic microwave background (CMB), shown in Figure 2. The slight temperature differences in the CMB correspond to changes in density indicative of BAOs. Due to complex interactions with secondary BAO resonances, the first, outermost BAO is the only one that would be consistent among all overdense regions. BAOs left a distinctive imprint on the distribution of matter in the universe, which we can now detect in the form of a "standard ruler" that provides critical insights into the universe's expansion history.

Importance of BAOs

BAOs are of particular interest because they offer an independent means to study the geometry of the universe and constrain cosmological parameters, such as the Hubble parameter. By precisely measuring the size of the BAO over different redshift scales, the rate of cosmic expansion over time and the properties of dark energy can be assessed. This makes BAOs a valuable tool in understanding the accelerated expansion of the universe, complementing measurements from other sources like supernovae and the CMB.

Existing Work for Detecting BAO Peaks

Baryon acoustic oscillations were first theoretically predicted by Sunyaev and Zeldovich (1970). By modelling the dynamics of the primordial plasma in the early universe, they showed that oscillations should occur until recombination, where they would effectively be frozen in place as radiation pressure would halt the expansion of the BAO. However, the BAO signal was not definitively found until much later. Following this theoretical prediction, early research conducted by Eisenstein et al. (2005) using luminous red galaxies (LRGs) between $0.16 < z < 0.47$ from the Sloan Digital Sky Survey (SDSS) showed the first promising result for discovering a BAO peak.

Eisenstein's model uses the Landy-Szalay estimator which we will adapt for our methods (see Methods section). This estimator uses a randomly generated simulated LRG samples with a comoving separation of roughly 100 h^{-1} Mpc (Landy and Szalay 1993). However, the results of this study are limited by the extent of the redshift range studied and the galaxies selected, which is why in our study, we decided to look at higher redshift ranges with quasars from the DESI dataset. Our data selection sample differs from what early research has produced but application of their mathematical model for detecting a BAO peak is still applicable on a first order approximation basis.

In order to supplement the observations made by SDSS, DESI began operations in 2019 to map out the universe in greater detail at low redshifts and find high-redshift objects to determine the nature of dark energy and measure the accelerated expansion of the universe. DESI uses an array of 5000 fiber-optic cables to observe target galaxies and classifies them based on their spectra. Using this method, DESI can detect emission line galaxies up to a redshift of 1.7 and Lyman-α quasars up to a redshift of 3.5. However, due to the relatively scarce amount of data at high redshifts compared to that at lower redshifts, the most recent study from DESI limited their analysis to bright galaxies and luminous red galaxies at redshifts below 0.5 and 1, respectively (Moon et al. 2023). Consequently, the high-redshift BAO peak from the DESI EDR remains undetected.

Methods

Data Collection and Preprocessing

The first 2 percent of data collected by DESI, was made public with the DESI EDR, with the rest of the data planned to be published once it completes its observation cycle in 2025. Once the rest of the data is released, we then have higher redshift ranges to work with for detecting BAO peaks in future work.

We used the NOIRLab DataLab website to collect the DESI EDR data due to the simplicity of running ADQL queries to compile all of the necessary data. We selected a redshift range of $2 < z < 3$ as past studies lack detail in this redshift range. A consequence of this redshift selection is the complete absence of non-quasars in the target object list, limiting the results of the study.

Once the data was downloaded as a .csv file, we preprocessed the data by removing columns that were not useful for the analysis, leaving the photometric ID, redshift, right ascension, and the declination. This was done to improve file processing time within the algorithm.

Correlation Function

The commonly used technique for calculating the correlation function across both simulated results (Huff et al. 2007) and from existing work of detecting BAO peaks both apply the Landy-Szalay estimator given by equation 1 below (Landy and Szalay 1993).

$$\xi(s) = \frac{DD(s) - 2DR(s) + RR(s)}{RR(s)}$$

Equation 1: Equation for the Landy-Szalay estimator, where $DD(s), RR(s)$ are the normalized autocorrelation functions for the galaxy sample and random sample, respectively, and $DR(s)$ is the cross-correlation function between the galaxy and random samples.

Before computing the four correlation functions above, we calculated the redshifts between each unique pair of objects were found using a method derived from Liske (2000), shown in Equations 2, 3, and 4 below. As the substitution for $q_1(z)$ provided by Liske (2000) assumes a universe where $\Omega_\Lambda = 0$, we derive Equation 4 from Sarath et al. (2022) assuming that the coefficient of bulk viscosity $\widetilde{\xi_1}$ and dimensionless coefficient e 0, which is a reasonable approximation. We assumed that $\Omega_M = 0.3$ and $\Omega_\Lambda = 0.7$ in a flat universe ($\Omega_k = 1$) when computing the distances.

$$z_2' = \frac{2P^2}{(q_1 - 2P^2)^2}\left(1 + q_1 - 2P^2 + \sqrt{\frac{q_1^2}{P^2} + 1 - 2q_1}\right)$$

$$P^2 = \left(\frac{1}{1+z_1}q_1\right)^2 \cdot 2\left(\left(\Sigma\left(\frac{\chi(z_2)+\chi(z_1)}{2}, 0\right)\right)^2 \sin^2\left(\frac{\alpha}{2}\right) + \left(\Sigma\left(\frac{\chi(z_2)-\chi(z_1)}{2}, 0\right)\right)^2 \cos^2\left(\frac{\alpha}{2}\right)\right)^{\frac{1}{2}}$$

$$q_1(z) = -1 + \frac{3(\Omega_M)(1+z)^3}{2\left((\Omega_M)(1+z)^3 + (1-\Omega_M)\right)}$$

Equations 2,3,4. Formulae derived from Liske (2000) and Sarath et al. (2022) for converting Earth-centered redshifts to redshift relative to one of the objects.

To generate the random sample for the correlation function, we created a spherical isotropic distribution of 16 times as many galaxies as the DESI data sample, with redshifts limited to the range of $2 < z < 3$. We then binned the computed redshift between each pair of objects into 5000 bins corresponding to different relative redshifts, from $z = 0$ to $z = 5$, spaced linearly, for each correlation function. Each real and simulated galaxy was given a weight of $\frac{1}{1+n(z)}$, where $n(z)$ is the number density of galaxies at a given redshift, computed via the formula $log\, n(z) = A(z) + \alpha(z)\big(M - \gamma(z)\big) + \beta(z)\big(M - \gamma(z)\big)^2 - exp\big(M - \gamma(z)\big)$, where $A(z), \alpha(z), \beta(z), \gamma(z)$ were fitted according to Torrey et al. (2015), and M represents the logarithm of the average mass of each galaxy, in agreement with the findings by Conselice et al. (2016). This formula is validated by Van der Wel et al. (2009), where the distribution of galaxies below $z = 2$ was determined.

Once the per-dataset correlation functions in redshift space were computed, we used Equation 1 to find the correlation function in redshift space, which was then converted into real space by converting each z to a distance using the formula shown in Equation 5 (Liske 2000, Hogg 2000).

$$\chi(z) = \frac{c}{100h}\int_1^{1+z} \frac{1}{\sqrt{\Omega_M x^3 + (1 - \Omega_M - \Omega_\Lambda)x^2 + \Omega_\Lambda}}\, dx$$

Equation 5. Integral allowing conversion from redshift to comoving distance in units of h^{-1}.

Results

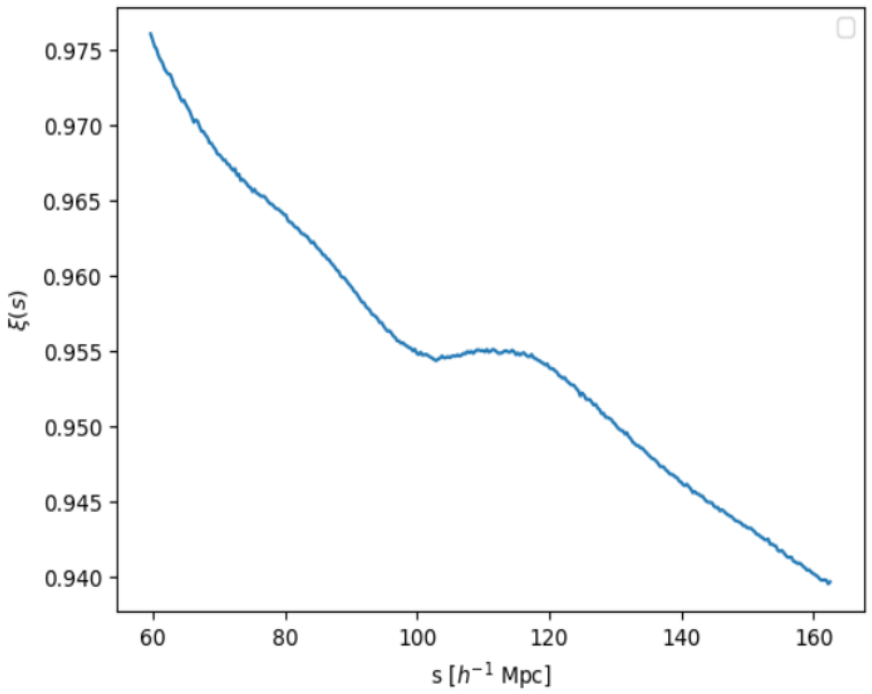

Figure 3. Correlation function obtained from the DESI EDR sample. A noticeable peak can be seen at roughly 110 h^{-1} Mpc.

By applying the data processing method and correlation function in our methods section, we were able to detect a peak in the correlation function as seen in Figure 3. To verify that the peak at roughly 110 h^{-1} Mpc is a genuine BAO peak, we computed the correlation function with the cosmological parameter $\Omega_\Lambda = 0$ to represent a matter-dominated universe. The result compared with the original graph is shown in Figure 4.

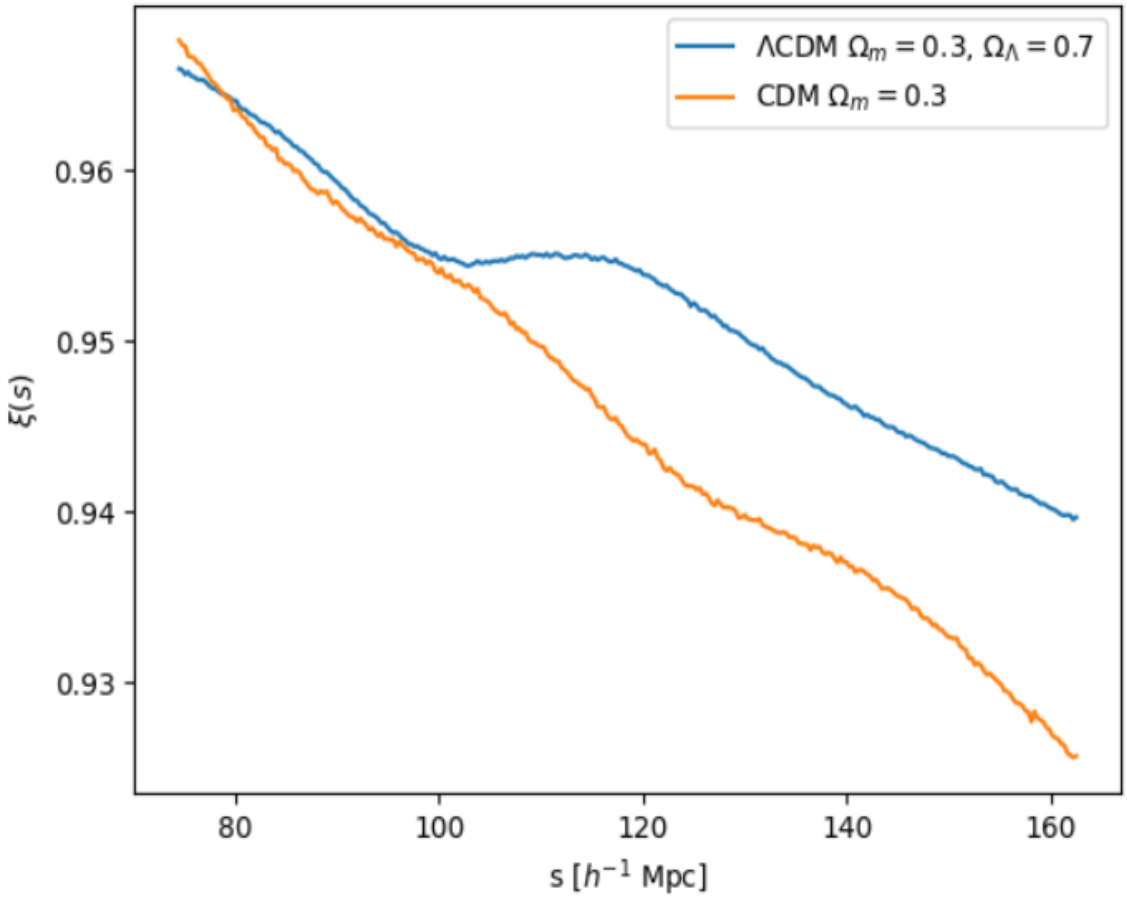

Figure 4. Correlation functions assuming $\Omega_m = 0.3$. $\Omega_\Lambda = 0.7$ for the blue graph and $\Omega_\Lambda = 0$ for the orange graph, the latter simulating a CDM universe.

The CDM correlation function lacks the acoustic peak because in a universe without dark energy, there would be no driving mechanism to expand the size of any existing BAOs to the observed separation. While it is apparent that the ΛCDM model indeed has a BAO peak while the CDM model does not, we elected to conduct a two-tailed paired t-test to verify the significance of this difference. The paired t-test was conducted over the range 74 h^{-1} Mpc to 163 h^{-1} Mpc, the area of interest for the BAO fitting. The final t-statistic of 24.312 with 299 degrees of freedom corresponds to a p-value of $4 \cdot 10^{-73}$, which are orders of magnitude lower than the significance value of $\alpha = 0.01$. Therefore, is highly likely that the peak found in Figure 4 is indeed the BAO peak.

Power Spectrum

Additionally, we a generated a power spectrum for the correlation function, which can be related to the correlation function using the equation $P(k) = \sqrt{\frac{2}{\pi}} \int_0^\infty s^2\, \xi(s) \left(\frac{\sin ks}{ks}\right) ds$ with the results shown in Figure 5 and Figure 6.

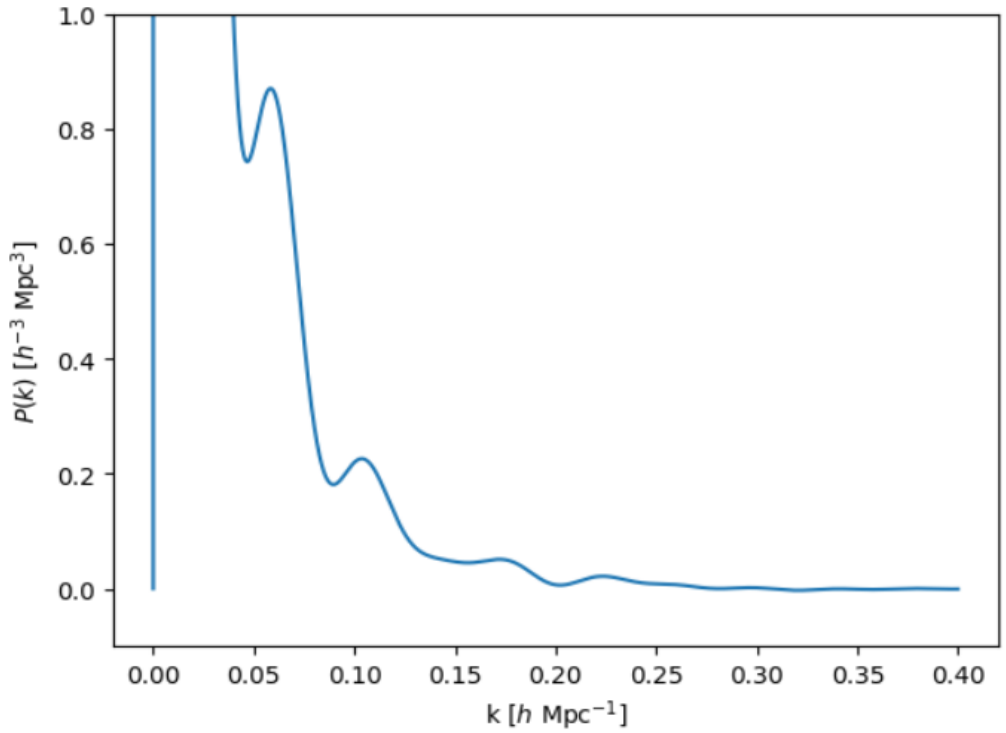

Figure 5. Power spectrum of the correlation function. There are several visible peaks in the wavenumber strengths.

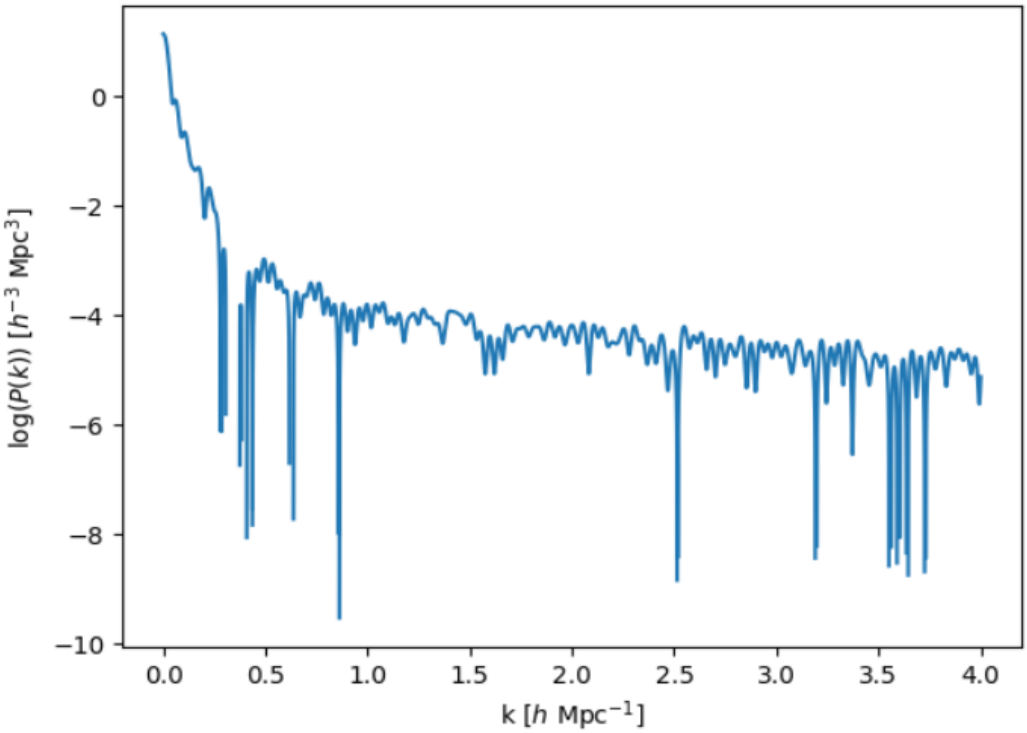

Figure 6. Full power spectrum of the correlation function. The logarithm of the power spectrum was taken to better display weak oscillations within the graph.

Based on the power spectrum shown in Figures 5 and 6, it is possible that the other peaks at higher wave-numbers indicate higher-order BAOs that were caused by resonances.

While this result appears very promising, there are a few errors associated with this method. For example, the correlation function was computed in redshift space for accuracy and then translated into real space, meaning that the equal spacing on the x-axis in redshift space would be lost after the conversion. Additionally, the formula for number density of galaxies assumed the mass for all galaxies to be $\log(M) = 10$, when in reality the masses of different galaxies can vary significantly from this chosen value.

Discussion

As seen in Figure 4 and the subsequent paired t-test, it is clear that the peak detected at 110 h^{-1} Mpc is a true BAO peak. This is significant as it shows the potential of the DESI survey for detecting BAO signals across the universe. As the EDR is only a small fraction of what the first data release will entail, it would be expected that the first data release would produce even better results compared to the first-order approximation presented here. Furthermore, due to the simplicity of the algorithm and its relatively simple parameter requirements, this algorithm possibly can easily be applied to data from other galactic surveys, including SDSS and the 2dF Galaxy Redshift Survey.

The detection of the BAO peak within this redshift range is important in refining the use of BAOs as a standard ruler, where the peak in real space may drift across several redshifts. By computing the distance between the Earth and a certain redshift, this value obtained via Equation 5 can be compared to the angular diameter of the BAO peak. This allows for the refining of cosmological parameters at the specified redshift, giving humans a better understanding of the evolution of the universe and allowing for further scrutiny on the current ΛCDM model.

Conclusion

The BAO peak within the DESI EDR between redshifts $2 < z < 3$ has been found and confirmed at a separation of 110 h^{-1} Mpc. The Landy-Szalay estimator was used to compute the correlation function in redshift space, with each pair of objects being weighted according to the number density of galaxies at the specified redshift. To find the distances between objects, the relative redshifts between two objects was computed and converted to a comoving distance using numerical integration.

The results of this study are limited primarily by a lack of affiliation with national labs, as this is a relatively surface-level exploration of the BAO peak within the DESI EDR. Additionally, there are several assumptions made when computing the correlation function. For example, the random sample was created as an isotropic distribution rather than simulating a universe lacking acoustic oscillations or a pure-CDM universe. Furthermore, the number density function was assumed to have a constant mass parameter as mass information for the target galaxies was not provided. Finally, the results of this study are limited to QSOs as the DESI EDR lacks non-QSO objects at high redshifts.

To improve the result of this study, better models for the random dataset used in the correlation function estimator, such as a mock catalog, could be used (Parihar et al. 2014, Eisenstein et al. 2005). Alternatively, n-body simulations beginning at photon decoupling running up to $z = 3$ could be performed to generate a random sample for the correlation function to accurately simulate the universe (Seo and Eisenstein 2005). Furthermore, a mass-dependent number density function for weighting each galaxy in the samples, could increase the accuracy of the weighting of galaxy samples (Iribarrem 2012).

In the future, further work could be done regarding this new method of studying BAOs within the DESI dataset. For example, cosmological parameters could be refined using the data obtained from this study, including the Hubble constant. As the Hubble constant is currently in tension from two measurements, a study using the correlation

function found here could be conducted to determine the Hubble parameter between the $2 < z < 3$ redshift range, adding to the existing database of Hubble constant calculations.

In addition to cosmological parameter refinement, the addition of new data points through the 2025 DESI full data release would enhance the results of this study. Because the DESI EDR covers only 2 percent of the entirety of the DESI survey, it would be expected that the results obtained from the full data release would provide more precise measurements for the BAO peak at this redshift range. The detection of the BAO signal within the DESI EDR at high redshifts provides critical insights on how our universe is evolving, adding to the global database of BAO detections across several surveys and redshift ranges.

Acknowledgments

I would like to thank my advisor for helping guide me with my project.

References

Chung, D. (2020). A unifying theory of dark energy, dark matter, and baryonic matter in the positive-negative mass universe pair: Protogalaxy and galaxy evolutions. *Journal of Modern Physics*, *11*(07), 1091-1122. https://doi.org/10.4236/jmp.2020.117069

Conselice, C. J., Wilkinson, A., Duncan, K., & Mortlock, A. (2016). The evolution of galaxy number density at z < 8 and its implications. *The Astrophysical Journal*, *830*(2), 83. https://doi.org/10.3847/0004-637x/830/2/83

De Sainte Agathe, V., Balland, C., Du Mas des Bourboux, H., Busca, N. G., Blomqvist, M., Guy, J., Rich, J., Font-Ribera, A., Pieri, M. M., Bautista, J. E., Dawson, K., Le Goff, J., De la Macorra, A., Palanque-Delabrouille, N., Percival, W. J., Pérez-Ràfols, I., Schneider, D. P., Slosar, A., & Yèche, C. (2019). Baryon acoustic oscillations at z = 2.34 from the correlations of Lyα absorption in eBOSS DR14. *Astronomy & Astrophysics*, *629*, A85. https://doi.org/10.1051/0004-6361/201935638

Eisenstein, D. J., Zehavi, I., Hogg, D. W., Scoccimarro, R., Blanton, M. R., Nichol, R., Scranton, R. C., Seo, H., Tegmark, M., Zheng, Z., Anderson, S. F., Annis, J., Bahcall, N., Brinkmann, J., Burles, S., Castander, F. J., Connolly, A., Csabai, I., Doi, M., Hennessy, G., Ivezić, Z., Kent, S., Knapp, G. R., Lin, H., Loh, Y., Lupton, R. H., Margon, B., McKay, T. A., Meiksin, A., Munn, J. A., Pope, A., Richmond, M. W., Schlegel, D., Schneider, D. P., Shimasaku, K., Stoughton, C., Strauss, M. A., SubbaRao, M., Szalay, A. S., Szapudi, I., Tucker, D. L., Yanny, B., & York, D. G. (2005) Detection of the Baryon Acoustic Peak in the Large-Scale Correlation Function of SDSS Luminous Red Galaxies. *The Astrophysical Journal, 633*(2), 560–574 https://doi.org/10.1086/466512

Hogg, D. W. (2000). Distance measures in cosmology. arXiv:astro-ph/9905116v4

Huff, E., Schulz, A. E., White, M., Schlegel, D. J. & Warren, M. S. (2007) Simulations of baryon oscillations. *Astroparticle Physics, 26*(6), 351–366. https://doi.org/10.1016/j.astropartphys.2006.07.007

Iribarrem, A. S., Lopes, A. R., Ribeiro, M. B., & Stoeger, W. R. (2012). Relativistic cosmology number densities and the luminosity function. *Astronomy & Astrophysics*, *539*, A112. https://doi.org/10.1051/0004-6361/201117535

Landy, S. D. & Szalay, A. S. (1993) Bias and Variance of Angular Correlation Functions. *The Astrophysical Journal, 412*(1), 64-71, https://doi.org/10.1086/172900 *The Astrophysical Journal, 412*(1), 64-71. https://doi.org/10.1086/172900

Liske, J. (2000). On the cosmological distance and redshift between any two objects. *Monthly Notices of the Royal Astronomical Society*, *319*(2), 557-561. https://doi.org/10.1111/j.1365-8711.2000.03874.x

Moon, J., Valcin, D., Rashkovetskyi, M., Saulder, C., Aguilar, J. N., Ahlen, S., Alam, S., Bailey, S., Baltay, C., Blum, R., Brooks, D., Burtin, E., Chaussidon, E., Dawson, K., de la Macorra, A., de M attia, A., Dhungana, G.,

Eisenstein, D., Flaugher, B., Font-Ribera, A., Forero-Romero, J. E., Garcia-Quintero, C., A Gontcho, S. G., Guy, J., Hanif, M. M. S., Honscheid, K, Ishak, M., Kehoe, R., Kim, S., Kisner, T., Kremin, A., Landriau, M., Le Guillou, L., Levi, M., Manera, M., Martini, P., McDonald, P., Meisner, A., Miquel, R., Moustakas, J., Myers, A., Nadathur, S., Neveux, R., Newman, J. A., Nie, J., Padmanabhan, N., Palanque-Delabrouille, N., Percival, W., Pérez Fernández, A., Poppett, C., Prada, F., Raichoor, A., Ross, A. J., Rossi, G., Samushia, L., Schlegel, D., Seo, H., Tarlé, G., Magana, M. V., Variu, A., Weaver, B. A., White, M. J., Yèche, C., Yuan, S., Zhao, C., Zhou, R., Zhou, Z., & Zou, H. (2023) First detection of the BAO signal from early DESI data, *Monthly Notices of the Royal Astronomical Society, 525*(4), 5406–5422. https://doi.org/10.1093/mnras/stad2618

Palanque-Delabrouille, N., & Yèche, C. (2021, May 17). *DESI starts its large spectroscopic survey for 5 years*. Irfu, Institute of research into the fundamental laws of the Universe. https://irfu.cea.fr/en/Phocea/Vie_des_labos/Ast/ast.php?t=fait_marquant&id_ast=4945

Parihar, P., Vogeley, M. S., Gott, J. R., Choi, Y., Kim, J., Kim, S. S., Speare, R., Brownstein, J. R., & Brinkmann, J. (2014). A topological analysis of large-scale structure, studied using the CMASS sample of SDSS-III. *The Astrophysical Journal*, *796*(2), 86. https://doi.org/10.1088/0004-637x/796/2/86

Sarath, N., Mohan, N., & Mathew, T. K. (2023). Running vacuum cosmology with bulk viscous matter. *Modern Physics Letters A*, *38*(20n21). https://doi.org/10.1142/s0217732323500992

Seo, H. & Eisenstein, D. J. (2005) Baryonic acoustic oscillations in simulated galaxy redshift surveys. *The Astrophysical Journal*, *633*(2), 575–588. https://doi.org/10.1086/491599

Sunyaev, R. A., & Zeldovich, Y. B. (1970). Small-scale fluctuations of relic radiation. *Astrophysics and Space Science*, *7*(1), 3-19. https://doi.org/10.1007/bf00653471

Torrey, P., Wellons, S., Machado, F., Griffen, B., Nelson, D., Rodriguez-Gomez, V., McKinnon, R., Pillepich, A., Ma, C., Vogelsberger, M., Springel, V., & Hernquist, L. (2015). An analysis of the evolving comoving number density of galaxies in hydrodynamical simulations. *Monthly Notices of the Royal Astronomical Society*, *454*(3), 2770-2786. https://doi.org/10.1093/mnras/stv1986

Van der Wel, A., Bell, E. F., Van den Bosch, F. C., Gallazzi, A., & Rix, H. (2009). On the size and comoving mass density evolution of early-type galaxies. *The Astrophysical Journal*, *698*(2), 1232-1243. https://doi.org/10.1088/0004-637x/698/2/1232